

Counterfactual Behavior Cloning: Offline Imitation Learning from Imperfect Human Demonstrations

SHAHABEDIN SAGHEB and DYLAN P. LOSEY, Virginia Tech, USA

Learning from humans is challenging because people are imperfect teachers. When everyday humans show the robot a new task they want it to perform, humans inevitably make errors (e.g., inputting noisy actions) and provide suboptimal examples (e.g., overshooting the goal). Existing methods learn by mimicking the exact behaviors the human teacher provides — but this approach is fundamentally limited because the demonstrations themselves are imperfect. In this work we advance offline imitation learning by enabling robots to extrapolate what the human teacher meant, instead of only considering what the human actually showed. We achieve this by hypothesizing that all of the human’s demonstrations are trying to convey a single, consistent policy, while the noise and sub-optimality within their behaviors obfuscates the data and introduces unintentional complexity. To recover the underlying policy and learn what the human teacher meant, we introduce *Counter-BC*, a generalized version of behavior cloning. Counter-BC expands the given dataset to include actions close to behaviors the human demonstrated (i.e., counterfactual actions that the human teacher could have intended, but did not actually show). During training Counter-BC autonomously modifies the human’s demonstrations within this expanded region to reach a simple and consistent policy that explains the underlying trends in the human’s dataset. Theoretically, we prove that Counter-BC can extract the desired policy from imperfect data, multiple users, and teachers of varying skill levels. Empirically, we compare Counter-BC to state-of-the-art alternatives in simulated and real-world settings with noisy demonstrations, standardized datasets, and real human teachers. Overall, we find that extrapolating what the human teacher meant — as opposed to rigorously following what the human actually demonstrated — leads to more proficient learning from humans. See videos of our work here: <https://youtu.be/XaeOZWtTt68>

CCS Concepts: • **Computing methodologies** → **Learning from demonstrations**.

Additional Key Words and Phrases: Imitation Learning, Behavior Cloning, Human-Robot Interaction

1 INTRODUCTION

Robots can learn new tasks by imitating human examples. Consider the system in Figure 1: by watching how a human plays air hockey, this robot arm should learn how to block and hit the puck. But one fundamental limitation when learning from humans is that people are imperfect teachers. Human demonstrations of the task will inevitably contain mistakes, noise, and suboptimal actions, particularly in real-world settings with inexperienced human operators. For instance, when teaching the robot how to play hockey the human might accidentally miss the puck, press the wrong buttons on the joystick, or take convoluted paths towards the target. These imperfect demonstrations are a problem because — when robots mimic suboptimal examples — they learn to perform the task incorrectly (e.g., only hitting the puck occasionally).

To advance learning from humans we need robots that imitate what the user actually *meant*, not just what the human *showed*. This is inherently challenging because the human is the teacher: the robot infers its task based on behaviors the human demonstrates. If we acknowledge that human teachers make mistakes, then how should the robot reason over their potentially incorrect demonstrations in order to extract the intended task? Recent research attempts to resolve this question by introducing additional human guidance [15, 21, 22, 24, 38, 39, 42–44, 47] and by iteratively testing policies in the environment [6, 7, 9, 16, 23, 34, 40, 41, 46]. Within these prior works the robot asks a human expert to label the quality of some or all of their demonstrations. If the

This work was supported in part by NSF Grant #2337884.

Authors’ address: Shahabedin Sagheb, shahab@vt.edu; Dylan P. Losey, losey@vt.edu, Virginia Tech, Department of Mechanical Engineering, 635 Prices Fork Rd, Blacksburg, VA, 24060, USA.

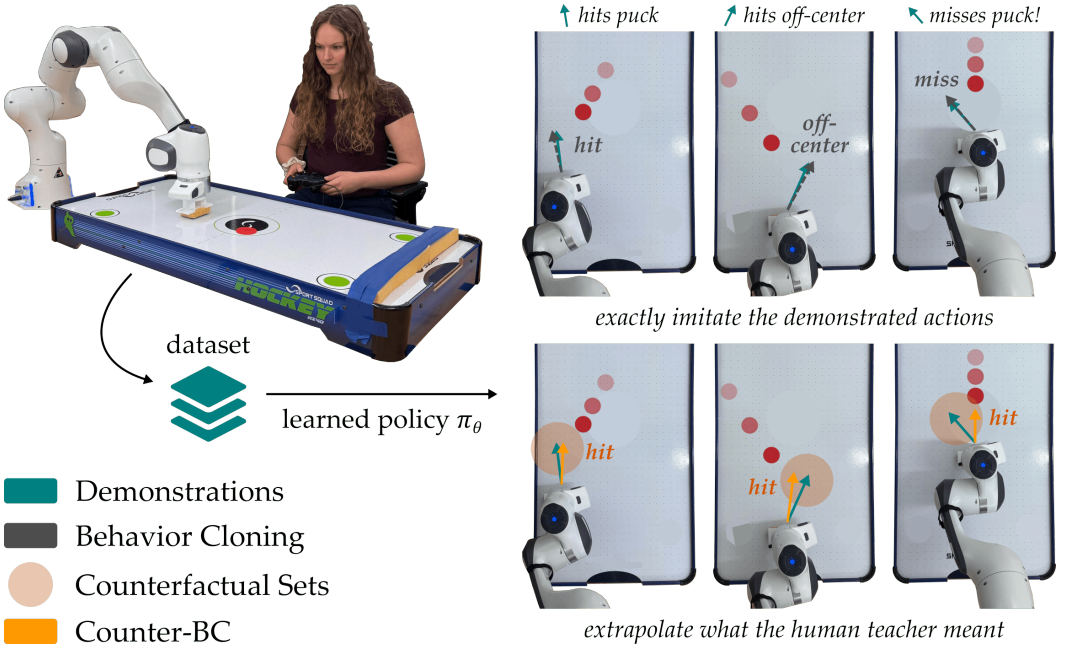


Fig. 1. Learning from imperfect human demonstrations. (Left) The human teaches a robot arm to play air hockey by showing examples of hitting the puck. (Right) The robot learns a control policy based on the human’s data. Within the state-of-the-art, the robot trains its policy offline to *exactly mimic* the actions demonstrated by the human — but this approach is fundamentally limited when human teachers make mistakes (like missing the puck). Counter-BC tries to imitate what the human *meant*, not necessarily what the human *showed*. More specifically, Counter-BC can modify the human’s demonstrations within counterfactual sets in order to match underlying behaviors across the entire dataset. This leads to robots that reach simple, consistent explanations of the human’s demonstrations, e.g., learning to hit the puck at every state.

robot knows which trajectories are proficient and which contain errors, then it can bias its learning to mimic the high-quality examples while ignoring low-quality behaviors. Unfortunately, asking people to watch and label demonstrations is time consuming and subjective — particularly for large-scale datasets that contain thousands of examples collected across diverse scenarios [4, 20, 35]. This brings us back to the fundamental problem: given only a dataset of human examples, how should the robot extract a control policy to autonomously complete the desired task?

In this work we propose a shift in perspective when learning from imperfect humans. Instead of trying to determine how good or bad each individual human demonstration is, we recognize that the human teacher has an underlying policy that all of their examples are trying to convey. The human’s imperfect teaching *obfuscates* this policy — i.e., makes it seem more complex or variable than it really is — by unintentionally adding noise and suboptimal actions into the dataset. To recover what the human actually meant, we accordingly hypothesize that:

*The robot learner should adjust the human teacher’s demonstrations
to reach a policy that simply and clearly explains their underlying trends.*

Applying this hypothesis we introduce *Counter-BC*, a variant of behavior cloning that learns from noisy and imperfect human teachers. Our offline imitation learning approach does not require additional human labels or knowledge about the environment. Instead, Counter-BC automatically expands the demonstrations to consider nearby actions. These *counterfactual actions* capture the

behaviors an imperfect human teacher might have been trying to show the robot. Returning to our hockey example in Figure 1, if the human inputs a motion that hits the puck off-center, the counterfactuals could include all actions within a radius Δ of that motion (including actions that miss the puck or hit the puck’s center). Equipped with counterfactual actions, the robot can now modify the human’s demonstrations (i.e., hypothesize that the human meant to show slightly different actions) in order to reach a simple and consistent explanation of the given dataset. This results in control policies that align with the underlying behaviors the human teacher intended to convey, instead of trying to copy the noisy and suboptimal actions the human actually demonstrated. For instance: a robot arm trained with Counter-BC learns to hit the puck at each iteration, even though our given demonstrations occasionally missed that puck.

Overall, this work is a step towards robots that learn proficient policies from datasets provided by everyday human teachers. We make the following contributions:

Generalizing Behavior Cloning. We analyze the loss function used to train the robot’s policy in standard behavior cloning algorithms, and show why that loss is ill-posed when learning from imperfect human data. To address this issue, we generalize the loss to include both counterfactual actions that expand the human’s demonstrations and a classifier that determines which counterfactual actions the robot learner should emulate. State-of-the-art approaches — including standard behavior cloning — can be viewed as simplified instances of this more general loss.

Deriving Counter-BC. Given the generalized loss function, we next derive our Counter-BC algorithm by selecting the counterfactuals and classifier. Our choices here cause the robot to learn a control policy which simultaneously does two things: i) the learned policy minimizes entropy to confidently output actions at each state, while ii) constraining those actions to remain close to the behaviors demonstrated by the imperfect human. We provide implementation details and public code for Counter-BC, and highlight that this offline imitation learning algorithm does not require any additional information beyond the human’s demonstrations.

Finding Simple Explanations. A key feature of Counter-BC is the size of the counterfactual set. Designers can tune this size along a continuous spectrum by adjusting its radius Δ . We theoretically and empirically prove that increasing Δ (i.e., making the counterfactual sets larger) causes the robot to learn simpler policies, but these policies may increasingly diverge from the behaviors the human provided. When learning from expert users, we decrease Δ to closely mimic the demonstrated actions; when learning from inexperienced users we increase Δ to extrapolate underlying patterns.

Testing with Synthetic Demonstrations. We compare Counter-BC to state-of-the-art baselines across multiple environments. Within these tests we first collect synthetic human demonstrations with controlled noise distributions (e.g., Gaussian, uniform). We then explore how effectively Counter-BC and the baselines learn the desired task as we vary the noise within the human’s demonstrations. In general, we find that Counter-BC outperforms existing methods regardless of what type of noise or suboptimal actions the synthetic human provides.

Learning from Real Humans. We conclude by learning from actual human data across simulated environments, standardized datasets, and an air hockey experiment. We again compare Counter-BC to existing offline imitation learning methods, and study how proficiently the robot learns the desired task based on examples from $N = 20$ human demonstrators. Our results indicate that robots which try to extrapolate what the human teacher meant (as opposed to copying or ignoring what the human actually did) are able to learn more effective policies from real human data.

2 RELATED WORK

Learning from noisy and imperfect human demonstrations is a core challenge for imitation learning [3, 27, 45]. Humans inevitably make errors when they show robots how to perform tasks — if robots

naively mimic these mistakes, they will learn to perform the tasks incorrectly. The emergence of large-scale datasets for robot learning has made this issue increasingly important. To collect vast amounts of data, systems such as [4, 20, 35] rely on multiple human teachers of varying skill and proficiency. Given a heterogeneous dataset, how should the robot extract the correct behavior?

Improving Human Teaching. One approach is to help the human become a better teacher. By giving the human offline guidance before they demonstrate the task, or real-time feedback during their demonstration, the robot may improve the quality of the human’s examples [11, 17, 31]. For instance, the robot can indicate when the human’s current trajectory deviates from previous behaviors. Related works have accordingly leveraged augmented reality [29], haptic interfaces [37], physical markers [12], or computer screens [14] to assist the human teacher. Once demonstrations are collected, the robot can also post-process the resulting data to filter out poor examples and human errors [8, 18]. Overall, these works are complementary but orthogonal to our efforts: instead of assisting the human, we will advance how the robot *learns* from a human-provided dataset.

A variety of learning algorithms have already been proposed for imperfect human demonstrations. Below we divide this related research into three groups: methods that rely on environment interactions, methods that rely on rankings, and methods that only consider the offline dataset.

Leveraging Environment Interactions. The first way in which robots can learn from noisy demonstrations is by extracting a reward [6, 9, 34] or discriminator [7, 40, 41, 46] from those demonstrations. The robot then interacts with the environment online (i.e., the robot arm attempts to complete the task) using reinforcement learning algorithms [6, 9, 34] or adversarial networks [7, 40, 41, 46]. Through these interactions the robot finds policies which maximize the reward, or which the discriminator cannot distinguish from expert human examples. One advantage of this paradigm is that — given ranked demonstrations — the robot can learn behaviors that are better than the best human demonstrations [6, 9]. But the downside is that this approach is *online*, and requires access to the environment dynamics through simulations or real-world rollouts. For practical implementation, we instead focus on imitation learning algorithms which are purely *offline*, and do not require any environment interactions during training.

Leveraging Supervised Labels. Some research achieves offline imitation learning from imperfect demonstrations by labeling (or scoring) the dataset. These labels reflect the relative quality of an example: e.g., a trajectory that goes precisely to the goal might be labeled as an “expert” demonstration and given a high score, while a trajectory that overshoots the goal could be labeled as “novice” and given a low score. Based on this labeled dataset, the robot learns a policy offline which aligns with high-quality demonstrations while down-weighting or ignoring low-quality inputs. The key challenge here is how to label the dataset; i.e., how to discern expert and novice demonstrations. When the robot has access to its reward function, this process is straightforward [16, 23]; trajectories with higher rewards are higher quality. More generally, recent works focus on settings where a portion of the dataset is labeled, and the rest is unlabeled [15, 21, 22, 24, 38, 39, 42–44, 47]. The exact way that the labels are collected can vary. For instance, in [38] it is assumed that a human has marked some subset of the data as “expert.” Alternatively, in [22] the human indicates the relative quality of a few demonstrations along a continuous or discrete scale. Regardless of how the labels are obtained, these works leverage the known labels to autonomously determine the quality of the remainder of the (unlabeled) dataset, and then train a policy to align with the high-quality examples. Of course, the downside to this framework is that labeling the demonstrations takes time and effort; a human expert must watch multiple demonstrations to grade their relative quality. We therefore seek a method which *does not require* any additional human inputs, rankings, or labels.

Leveraging Only Human Demonstrations. Most related to our proposed approach are methods that learn a policy given only the human’s noisy and imperfect demonstrations. These methods

do not assume access to environment interactions or supervised labels; instead, they seek to extrapolate what the human meant based only on trends in the human’s data. In [30] the authors modify behavior cloning so that the robot’s learned policy concentrates on the modes of the human’s demonstrations. Put another way, the robot learns to consistently mimic the behaviors which are most common in the dataset. When these modes are correct, the robot learns the desired task — but if the majority of the dataset is not expert behavior, [30] falls short. Similarly, [2] assumes that human demonstrations are high-quality when those demonstrations output a consistent action at a given state, and low-quality when the demonstrated actions have high variance. We will experimentally compare our proposed algorithm to both of these state-of-the-art baselines. In general, the key difference between our method and [30] or [2] is that we enable the robot to incorporate counterfactuals (i.e., actions that the imperfect human could have intended, but did not actually demonstrate) to build a control policy that consistently explains the data. We note that [33] also uses counterfactuals, but applies them in settings where the robot has access to expert labels.

3 PROBLEM FORMULATION

We consider scenarios where a robot is learning a new task from one or more human teachers. Offline, the human teacher(s) provide examples of how the robot should complete the desired task. Because humans are noisy and imperfect, their demonstrations will inevitably contain mistakes (i.e., suboptimal actions that they do not want the robot to imitate). The robot’s goal is to learn how to perform the task correctly, despite imperfect or suboptimal examples in the dataset.

Robot. Let $s \in \mathcal{S}$ be the system state and let $a \in \mathcal{A}$ be the robot’s action. For instance, within our motivating example s contains the robot’s joint position, end-effector pose, and an image of the hockey table; the action a is the robot’s joint velocity. The robot’s actions cause the system state to transition according to its dynamics. We do not assume access to these environment dynamics. Put another way, when the robot arm moves to hit the hockey puck, the robot cannot explicitly model or simulate of how the puck will respond to its actions.

Human. The human has in mind a task they want the robot to learn. To teach the robot, the human demonstrates how to complete that task. Prior works have established multiple forms of demonstration: the human might kinesthetically guide the robot through the desired motion [1], teleoperate the robot along a trajectory [26], or employ graphical user interfaces, augmented reality, or natural language inputs to indicate the correct action at various states [10]. Regardless of how they are collected, the human’s demonstrations result in a dataset \mathcal{D} of examples. Within this dataset the human teacher labels each system state s with an action a , such that $\mathcal{D} = \{(s_1, a_1), \dots, (s_n, a_n)\}$ is a collection of n state-action pairs. In our experiments we will focus on *offline datasets* (i.e., datasets collected prior to robot learning), but our approach also applies to settings where the human shows new state-action pairs online as the robot attempts to complete its task [32].

It is inevitable that the human will make mistakes when giving demonstrations. These mistakes may occur because the task is hard to perform, because the human is distracted or moving quickly, or because it is challenging to perfectly orchestrate the motion of a dexterous robot arm [5, 11, 25, 31]. To formulate teaching errors we define a^* as the *ideal action* the human meant to show the robot. If the human acted perfectly, they would have provided an ideal dataset $\mathcal{D}^* = \{(s_1, a_1^*), \dots, (s_n, a_n^*)\}$. In practice, however, the noisy human actually demonstrates suboptimal actions a :

$$a = a^* + \epsilon, \quad \epsilon \sim P(\cdot \mid s) \quad (1)$$

where ϵ is the error between the ideal action a^* and the actual action a . At each state in the collected dataset \mathcal{D} this action error is sampled from some unknown distribution $P(\epsilon \mid s)$.

Policy. Despite the noise inherent in the human’s examples, the robot’s objective is to learn a *control policy* that autonomously completes the demonstrated task. This control policy is a mapping from observed states s to robot actions a :

$$a \sim \pi_\theta(\cdot \mid s) \quad (2)$$

We instantiate the control policy π as a model (e.g., a neural network) parameterized by weights $\theta \in \Theta$. In practice, there are three different control policies that our formulation must consider: i) the ideal policy π^* that the human is trying to convey to the robot, ii) the noisy and imperfect policy π that the human actually follows when providing demonstrations, and iii) the robot’s learned policy π_θ . Ideal actions a^* and the ideal dataset \mathcal{D}^* are sampled from the ideal policy π^* , while the demonstrated actions $a = a^* + \epsilon$ and the collected dataset \mathcal{D} are sampled from the imperfect policy π . We emphasize that the robot does not know either π^* or π . Instead, based on the dataset \mathcal{D} induced by π , the robot seeks to learn a control policy π_θ that matches the ideal policy π^* .

Behavior Cloning. Recent works have found that methods founded on behavior cloning are a promising way to learn π_θ from suboptimal demonstrations [13, 27, 28, 30]. To better understand these baselines — and set the stage for our own approach — we here derive the loss function used to train the robot’s policy in behavior cloning algorithms. Intuitively, the robot seeks to learn θ such that its control policy π_θ matches the expert policy π^* . We can measure the distance between distribution π_θ and distribution π^* using Kullback–Leibler (KL) divergence. Applying KL divergence to conditional probabilities, we reach:

$$D_{KL}(\pi^*, \pi_\theta) = C - \int_{s \in \mathcal{S}} \int_{a \in \mathcal{A}} \left[\rho^*(s) \pi^*(a \mid s) \log \pi_\theta(a \mid s) \right] \quad (3)$$

$$= C - \mathbb{E}_{s \sim \rho^*(\cdot), a^* \sim \pi^*(\cdot \mid s)} \left[\log \pi_\theta(a^* \mid s) \right] \quad (4)$$

where C is a constant term that does not depend on θ , and $\rho^*(s)$ is the distribution over states induced by the expert policy $\pi^*(a \mid s)$. Accordingly, to reduce the error between π_θ and π^* the robot should update θ to minimize the right side of Equation (4). This leads to the loss function:

$$\mathcal{L}(\theta) = \mathbb{E}_{s \sim \rho^*(\cdot), a^* \sim \pi^*(\cdot \mid s)} \left[-\log \pi_\theta(a^* \mid s) \right] \quad (5)$$

Approximating this expectation by sampling from the expert policy, Equation (5) becomes:

$$\mathcal{L}(\theta) \propto \sum_{(s, a^*) \in \mathcal{D}^*} \left[-\log \pi_\theta(a^* \mid s) \right] \quad (6)$$

which forms the standard loss function for behavior cloning algorithms [3, 19, 30]. Training the model weights θ to minimize the loss in Equation (6) corresponds to learning a control policy π_θ that matches the expert policy π^* across states in the dataset.

Unfortunately, this standard behavior cloning loss has a significant issue when applied to noisy and imperfect data. Based on the derivation in Equation (6), to learn the intended policy the robot should reason over the ideal dataset \mathcal{D}^* . But in reality the robot does not have access to \mathcal{D}^* . Instead, humans provide \mathcal{D} — a dataset with noisy, imperfect, and suboptimal examples. One naive solution is just to replace \mathcal{D}^* with \mathcal{D} in Equation (6) and then train the robot’s policy (we test this baseline in our experiments). However, doing so means that our robot is being trained to imitate incorrect human examples as opposed to the desired behaviors. We must therefore develop an approach that modifies Equation (6) to extrapolate from the noisy human demonstrations in dataset \mathcal{D} .

4 COUNTERFACTUAL BEHAVIOR CLONING

In this section we present counterfactual behavior cloning (Counter-BC), a modification of behavior cloning designed to learn from noisy and imperfect human demonstrations. Our core hypothesis is that human teachers have in mind an underlying control policy they are trying to convey, and the noise in their demonstrations obfuscates this control policy by introducing additional variation and complexity. As such, robot learners should reason over the human’s demonstrations — and even modify those demonstrations — in order to reach a *simple explanation* of the given data. Counter-BC achieves this by expanding the demonstrations to include counterfactual actions: i.e., actions that the suboptimal human did not actually demonstrate, but may have intended to show the system. The robot learns a policy that minimizes entropy over these counterfactual actions; this policy is a *simple explanation* because the learned function is confident about what action to take at each state in the dataset (preventing the robot from overfitting to the variability and complexity introduced by the human’s noisy behavior). In Section 4.1 we expand the standard behavior cloning loss to now account for counterfactual actions, and explain how this generalizes methods from prior work. Next, in Section 4.2 we derive the key terms of the new loss function, and show how the resulting policy selects counterfactuals that lead to minimal entropy. Finally, in Section 4.3 we outline the Counter-BC algorithm and practical implementation details.

4.1 Generalizing the Loss with Counterfactuals

Human teachers inevitably provide imperfect and suboptimal demonstrations. In Equation (1) we formulated the impact of those demonstrations: instead of showing actions a^* (sampled from the ideal policy π^*), everyday users input actions a (sampled from their suboptimal policy π). Put another way, at each (s, a) pair in the dataset \mathcal{D} the human may have actually meant to show some other behavior. Our proposed method captures these alternative actions through *counterfactual sets*. Given a state-action pair, let $a' \in C(s, a)$ be the set of counterfactual actions that the human could have intended to demonstrate. By leveraging counterfactual sets C we can expand the standard behavior cloning loss from Equation (6) into a more general form:

$$\mathcal{L}(\theta) \propto \sum_{(s,a) \in \mathcal{D}} \sum_{a' \in C(s,a)} \left[-R(s, a') \cdot \log \pi_\theta(a' | s) \right] \quad (7)$$

Here C iterates through the actions the human might have wanted to show, and $R(s, a) \in [0, 1]$ classifies these hypothetical actions along a continuous spectrum from expert ($R \rightarrow 1$) to non-expert ($R \rightarrow 0$). Equation (7) reduces to Equation (6) when: i) the counterfactuals include the ideal action $a^* \in C(s, a)$ at each state, and ii) $R(s, a) = 1$ for $a = a^*$, and $R(s, a) = 0$ otherwise. Introducing counterfactual actions is a shift in the robot’s perspective: instead of strictly learning to match the behaviors in \mathcal{D} demonstrated by the imperfect human teacher, now the robot can learn to mimic actions in $C(s, a)$ which the human never actually showed.

We highlight that the loss functions used by related works can also be viewed as simplifications of Equation (7). As summarized below, we reach these simplifications by making different choices for the counterfactual sets C or the classifier R in Equation (7):

- **Behavior cloning** [19]: $C(s, a) = \{a\}$, $R(s, a) = 1$ for all states.
- **Advantage-filtered behavior cloning** [16, 23]: $C(s, a) = \{a\}$, $R(s, a)$ is based on the advantage function or value associated with each state-action pair.
- **Discriminator-weighted behavior cloning** [42]: $C(s, a) = \{a\}$, $R(s, a)$ is a discriminator that assigns $R(s, a) \rightarrow 1$ to expert behavior and $R(s, a) \rightarrow 0$ to novice behavior.
- **ILEED** [2]: $C(s, a) = \{a\}$, $R(s, a)$ is the expertise level of the current human teacher where $R(s, a) \rightarrow 1$ when the human is an expert at the current state.

- **Sasaki and Yamashina [30]:** $C(s, a) = \{a\}$, $R(s, a) = \pi_{prev}(a \mid s)$ is the learned control policy from the previous training iteration.

One trend we observe is that — across each of these state-of-the-art methods — the robot always sets $C(s, a) = \{a\}$. This means that no actions besides the ones demonstrated by the human teacher can be explicitly treated as “expert” behavior (i.e., the robot does not reason over counterfactuals). As we will show, using counterfactuals is a fundamental change that enables the robot to interpret and explain the human’s demonstrations in ways not available when the system is constrained to only imitating ($R \rightarrow 1$) or ignoring ($R \rightarrow 0$) the behaviors provided by the human teacher.

4.2 Learning Policies that Consistently Explain the Counterfactuals

Given the generalized loss in Equation (7), our next steps are to select the counterfactual set C and classifier R used by our algorithm. Our choices of C and R should enable the robot learner to reason over the counterfactuals and reach a simple explanation of the underlying control policy.

Counterfactual Set. The counterfactual set accounts for noise and error in the human’s demonstrations by considering alternative actions that are close to the human’s actual behavior. For each $(s, a) \in \mathcal{D}$, let $C(s, a)$ contain all actions within a radius Δ of the demonstrated a :

$$C(s, a) = \{a' \mid \|a - a'\| - \Delta \leq 0\} \quad (8)$$

The radius $\Delta \geq 0$ in Equation (8) is a hyperparameter specified by the designer. If the robot is learning from an expert human teacher, the designer should set $\Delta \rightarrow 0$ since it is likely that the ideal action a^* is close to the expert’s demonstrated action a (i.e., the robot learner should trust the expert’s examples). By contrast — if the robot is learning from a novice teacher — the designer should increase $\Delta \rightarrow 2a_{max}$, where a_{max} is the magnitude of the largest action. Increasing Δ enables the robot to treat a larger range of actions as if they were the human’s intended behavior (i.e., although the human showed a , the robot thinks the human meant a').

Classifier. The classifier $R : \mathcal{S} \times \mathcal{A} \rightarrow [0, 1]$ determines which actions the control policy should emulate. Given a proposed counterfactual a' , increasing $R(s, a')$ indicates that a' is likely the intended human action. Interesting, we have already introduced a term that operates similarly to $R(s, a)$: the control policy $\pi_\theta(a \mid s)$ estimates the likelihood that a given action is part of the desired policy at state s . Recognizing this alignment, we define the classifier as a restriction of probability distribution π_θ with support over the counterfactual set:

$$R(s, a) = \hat{\pi}_\theta(a \mid s), \quad \hat{\pi}_\theta(a \mid s) = \frac{\pi_\theta(a \mid s)}{\sum_{a' \in C(s, a)} \pi_\theta(a' \mid s)} \quad (9)$$

Because the normalizer of $\hat{\pi}_\theta$ considers only the counterfactual set C , by definition $\hat{\pi}_\theta$ is a probability distribution that sums to one across the counterfactuals. Put another way, $R(s, a')$ in Equation (9) expresses the probability that counterfactual a' is really the action a^* the human teacher meant to demonstrate. For instance: in the special case where $C(s, a) = \{a\}$ and the robot does not consider counterfactuals, then $R(s, a) = 1$ and the robot is confident that the demonstrated action a is the intended action a^* . In what follows we will prove that this choice for classifier R (when combined with counterfactual sets C) biases the robot learner towards policies that provide simple explanations for the human’s noisy demonstrations.

Counter-BC Loss. To derive the loss function for Counter-BC we plug Equation (8) and Equation (9) back into Equation (7). Starting with our given choices of the counterfactual set and classifier, and

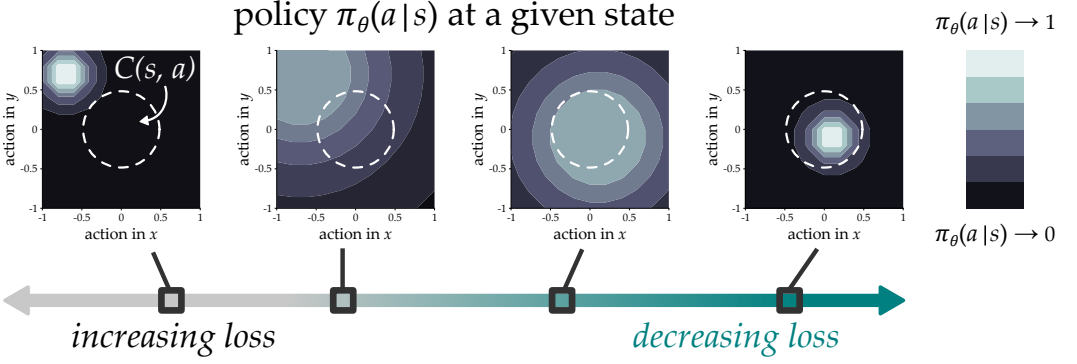


Fig. 2. Visualizing the loss in Equation (13) for a single state. Here the actions are two dimensional (i.e., in an x - y plane), and the demonstrated human action is at the origin. The counterfactual set lies within the dashed white circle ($\Delta = 0.5$). We show the probability distribution over actions for four different policies $\pi_\theta(a | s)$, where lighter regions indicate that the action is more likely. (Far Left) The maximum loss occurs when the policy confidently predicts an action outside the counterfactual. (Far Right) The minimum loss occurs when policy confidently predicts an action inside the counterfactual. Note that the predicted action does not need to be the demonstrated action; specifying any action within $C(s, a)$ can minimize the proposed loss.

then manipulating the terms, we eventually reach the cross entropy between $\hat{\pi}_\theta$ and π_θ :

$$L(\theta) \propto \sum_{(s,a) \in \mathcal{D}} \sum_{a' \in C(s,a)} \left[-\hat{\pi}_\theta(a' | s) \cdot \log \pi_\theta(a' | s) \right] \quad (10)$$

$$= \sum_{(s,a) \in \mathcal{D}} \sum_{a' \in C(s,a)} \left[-\hat{\pi}_\theta(a' | s) \cdot \log \frac{\pi_\theta(a' | s) \cdot \hat{\pi}_\theta(a' | s)}{\hat{\pi}_\theta(a' | s)} \right] \quad (11)$$

$$= \sum_{(s,a) \in \mathcal{D}} \sum_{a' \in C(s,a)} \left[-\hat{\pi}_\theta(a' | s) \cdot \log \hat{\pi}_\theta(a' | s) + \hat{\pi}_\theta(a' | s) \cdot \log \frac{\hat{\pi}_\theta(a' | s)}{\pi_\theta(a' | s)} \right] \quad (12)$$

$$= \sum_{(s,a) \in \mathcal{D}} H(\hat{\pi}_\theta | s, C(s,a)) + D_{KL}(\hat{\pi}_\theta, \pi_\theta | s, C(s,a)) \quad (13)$$

Here H is the conditional entropy over the restricted policy's actions given state s and counterfactual set C , and D_{KL} is the KL divergence between $\hat{\pi}_\theta$ and π_θ given state s and counterfactual set C . In practice, minimizing Equation (13) does two things. The first term drives our restricted policy $\hat{\pi}_\theta$ to have low entropy over the counterfactual set. The second term forces the robot's full policy π to match the restricted policy $\hat{\pi}_\theta$. Putting these terms together means that the robot will learn a policy π_θ that confidently outputs actions (i.e., minimizes entropy), while constraining those actions to be close to the behaviors demonstrated by the imperfect human.

To better visualize this loss function we provide an example in Figure 2. The loss is *highest* when the policy π_θ confidently predicts an action outside of the counterfactual set (far left). Conversely, the loss is *lowest* when π_θ confidently predicts an action within $C(s, a)$ (far right).

Intuition. Why is this loss function a good choice when learning from imperfect and noisy human demonstrations? Viewed at a single state s , minimizing Equation (13) results in a robot policy $\pi_\theta(a | s)$ that stochastically outputs an action $a \in C(s, a)$. Viewed across the entire dataset \mathcal{D} of state-action pairs, minimizing Equation (13) searches for a function that can confidently output actions in C at each individual state. This policy seeks to *explain* the human's data, and can *modify* the expert actions (i.e., change the selected counterfactual) in order to reach a more

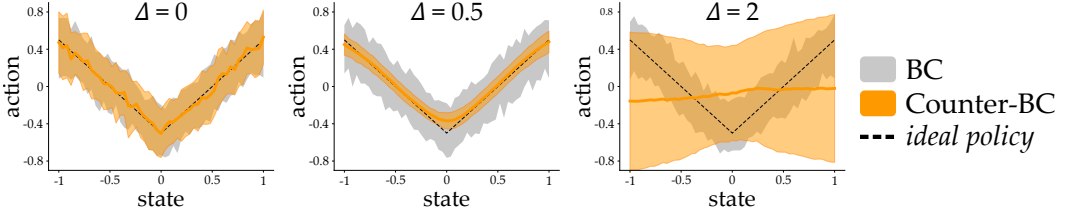


Fig. 3. Recovering the underlying function with Counter-BC. In a 1-dimensional environment the simulated human noisily demonstrates the absolute value function $a = |s| - 0.5 + \epsilon$, where $\epsilon \sim \mathcal{U}(-0.5, +0.5)$. We plot the robot’s learned policy averaged across 50 runs; shaded regions show the standard deviation. With behavior cloning (BC) the robot tries to precisely match the noisy data, resulting in a more complex explanation of the human’s demonstrations. (From left to right) Counter-BC with different values of hyperparameter Δ . Increasing Δ causes Counter-BC to recover increasingly simple explanations of the data by reasoning over larger counterfactual sets, but the resulting policies may diverge from the human’s examples.

efficient explanation of the dataset. Overall, the design of Equation (13) formalizes our hypothesis that there is an underlying function behind the human’s behaviors, and the robot may need to tweak the dataset in order to remove suboptimal actions and recover that intended function.

In Figure 3 we show an instance of using the Counter-BC loss to recover the underlying task — here a simulated human is demonstrating the absolute value function. Within this example we also highlight how tuning Δ affects the recovered policy. In general: *increasing Δ means the robot will recover a simpler function, but this function may increasingly diverge from the dataset*. When hyperparameter $\Delta \rightarrow 0$ then $C(s, a) = \{a\}$ and minimizing Equation (13) is equivalent to standard behavior cloning. Hence, as $\Delta \rightarrow 0$ the robot learns a policy that is sufficiency complex to match the given state-action pairs as precisely as possible. At the other extreme, when $\Delta \rightarrow 2a_{max}$ the counterfactual set is equal to the entire action set $C(s, a) = \mathcal{A}$. This in turn means that $\hat{\pi}_\theta = \pi_\theta$ in Equation (9), and Equation (10) becomes the conditional entropy of $\pi_\theta(a | s)$. Robots can minimize this conditional entropy with any deterministic function that outputs a consistent action at each state — for example, simply outputting a line in Figure 3. Accordingly, as $\Delta \rightarrow 2a_{max}$ the robot can fit the provided dataset with increasingly simplistic but inaccurate policies.

4.3 Implementation

Equipped with our understanding of the loss function we are now ready to present Counter-BC (see Algorithm 1). Counter-BC is an offline imitation learning approach that inputs a dataset of state-action pairs \mathcal{D} and the designer-specified hyperparameter Δ . During training Counter-BC learns a control policy with parameters θ to minimize Equation (10): this training phase does not require any human labels or environment interactions. Code for implementing Counter-BC is located here: <https://github.com/VT-Collab/Counter-BC>

In the experiments reported below we instantiate π_θ as a Gaussian policy with independent covariance. This policy is constructed from a fully connected neural network with two hidden layers and $\text{ReLU}(\cdot)$ activation functions. Actions are sampled from the policy using the reparameterization trick. To train the policy network we employ an Adam optimizer; unless otherwise stated, the hidden layers are of size 256 and the learning rate is $1e^{-3}$.

5 SIMULATIONS

In this section we compare Counter-BC to state-of-the-art alternatives in simulated environments. Actual participants and synthetic users provide demonstrations within each environment, and we leverage behavior cloning variants to try and recover the intended task from these imperfect

Algorithm 1 Counterfactual Behavior Cloning (Counter-BC)

```

1: Input dataset  $\mathcal{D} = \{(s_1, a_1), \dots, (s_n, a_n)\}$ 
2: Initialize control policy  $\pi_\theta(a | s)$  with weights  $\theta$ 
3: Specify the radius  $\Delta \geq 0$  used for sampling counterfactual actions
4: Sample counterfactual actions  $a' \in C(s, a)$  for each  $(s, a) \in \mathcal{D}$  ▷ Equation (8)
5: for epoch  $\in 1, 2, \dots, K$  do
6:    $\mathcal{L}(\theta) \leftarrow 0$  ▷ Initialize loss
7:   for  $(s, a) \in \mathcal{D}$  do
8:      $\log \pi_\theta \leftarrow [\log \pi_\theta(a' | s) \text{ for each } a' \in C(s, a)]$  ▷ Compute vector of length  $|C(s, a)|$ 
9:      $\hat{\pi}_\theta \leftarrow \text{softmax}(\log \pi_\theta)$  ▷ Equation (9)
10:     $\mathcal{L}(\theta) \leftarrow \mathcal{L}(\theta) - \hat{\pi}_\theta \cdot \log \pi_\theta$  ▷ Equation (10) with dot product between vectors
11:   end for
12:    $\theta \leftarrow \theta - \alpha \nabla_\theta \mathcal{L}(\theta)$  ▷ Update model weights to minimize loss
13: end for
14: Return trained control policy  $\pi_\theta(a | s)$ 

```

datasets. Our simulations explore i) how different types of noise and suboptimality affect the learner’s performance, ii) how the learner’s behavior changes as the amount of data varies, iii) how the level of noise in the human’s demonstrations impacts the learner, and finally iv) how adjusting hyperparameter Δ alters results with Counter-BC.

Environments. We selected four different environments to perform our simulations: *Intersection*, *Cartpole*, *Car Racing*, and *Robomimic*. Images of the environments are shown in Figure 4. Overall, these environments and tasks span different levels of complexity — from balancing a one-DoF inverted pendulum, to driving a vehicle based on RGB images, to controlling a robot arm that grasps and manipulates objects. In order to collect real human demonstrations, we needed to choose environments where humans can actually control the ego agent (i.e., teleoperate the robot). We also tried to pick environments that were consistent with related works, and leveraged existing datasets for learning from imperfect humans. Below we briefly summarize each environment.

Intersection. A multi-agent driving task from [28]. Two cars are crossing an intersection: the ego agent (which is controlled by a simulated or real human) and another agent (which is fully automated, and updates its motion in response to the ego agent). Both vehicles are attempting to reach their respective goals on the opposite side of the intersection while avoiding collisions with one another. The state $s \in \mathbb{R}^4$ includes the x - y position of both cars, and the action $a \in \mathbb{R}^2$ updates the position of the ego agent. The performance of the robot learner is measured by its total reward across an interaction; this reward is the negative of Equation (12) in [28].

Cartpole. A standard environment for robot learning [36]. The state $s \in \mathbb{R}^4$ captures the pose of a cart and attached pendulum, and actions $a \in \mathbb{R}^1$ move the cart left or right along a continuous action space in order to balance the inverted pendulum. The robot’s performance is measured by the number of timesteps the agent can keep the pendulum from falling over (up to a maximum of 200 timesteps). Related papers on learning from noisy human demonstrations have leveraged this environment or similar variations of the inverted pendulum problem [9, 33, 34, 43, 47].

Car Racing. A single-agent driving along a randomly generated road [36]. Unlike our other environments — where the robot has direct access to the system pose — here the state s is a 96×96 RGB image of the scene. The learner must map this visual input to continuous actions $a \in \mathbb{R}^3$ that

steer, accelerate, and brake. Humans provide demonstrations where they try to quickly advance while keeping the car on the road; the learner’s performance is measured by the distance traveled.

Robomimic. An existing dataset for learning robot manipulation tasks from real human demonstrations [27]. The dataset includes multiple tasks: we implement the *Can* task and *Multi-Human* dataset. In this task a FrankaEmika robot arm reaches to grasp a cylindrical can, carry it, and then drop it in the appropriate bin. The system state $s \in \mathbb{R}^{23}$ includes the robot’s pose, the can’s pose, and the can’s pose relative to the robot arm. Actions $a \in \mathbb{R}^7$ move the robot’s end-effector and actuate its gripper. The multi-human dataset includes 300 *Can* demonstrations collected from six different humans: two “better” operators, two “okay” operators, and two “worse” operators. Similar to [2, 22, 44], we directly leverage this existing multi-human dataset; no additional or synthetic demonstrations are collected for this environment. Performance is measured by the percentage of trials where the robot learner successfully completes the entire manipulation task.

Human Demonstrations. In *Intersection*, *Cartpole*, and *Car Racing* environments we collected real and synthetic human demonstrations. Within the synthetic demonstrations we injected different types of controlled noise or suboptimal behaviors. A list of demonstrators is provided below:

- **Real Humans.** We recruited $N = 20$ in-person participants (3 female, average age 24 ± 4 years) to teleoperate the ego agent. Participants provided informed written consent following university guidelines (IRB #23-1237). After practicing the tasks for up to five minutes, users provided demonstrations to convey the desired behavior in each environment.
- **Uniform.** Synthetic humans demonstrated the task by sampling actions according to Equation (1), where a^* is the optimal action that maximizes task performance and P is a uniform distribution: $\epsilon \sim \mathcal{U}(-\sigma, \sigma)$. Intuitively, these simulated human teachers had uniform noise added to their demonstrations.
- **Gaussian.** Synthetic humans sampled actions according to Equation (1), where a^* is the optimal action and P is an unbiased Gaussian distribution: $\epsilon \sim \mathcal{N}(0, \sigma^2)$.
- **Random.** With probability $1 - \sigma$ the demonstrator provides the optimal action so that $a = a^*$. Otherwise the synthetic human injects uniform noise: $\epsilon \sim \mathcal{U}(-\sigma, \sigma)$.

We emphasize that collecting actual human data is critical since the purpose of our approach is to learn from humans; *synthetic data may never capture the types of mistakes that real users make*. At the same time, testing with synthetic data is theoretically useful because it provides evidence about which noise distributions are most advantageous or challenging for each method.

Learning Algorithms. Given a dataset \mathcal{D} of state-action pairs provided by the real or synthetic human, the robot used offline imitation learning to train a policy π_θ . We compared policies learned with **Counter-BC** (Algorithm 1) to three state-of-the-art baselines for learning from noisy humans.

- **BC** [19]: Standard behavior cloning. The robot trains a Gaussian policy to try and exactly match the actions demonstrated by the human teacher.
- **ILEED** [2]: A behavior cloning variant that estimates the expertise of multiple teachers at different states. This approach is not directly applicable to our setting, since we do not know which datapoints belong to which human teacher. We therefore modify [2] to train the expertise level $\rho_\phi(s) \rightarrow [0, 1]$ purely as a function of the state. This corresponds to a learner that sets $R(s, a) = \rho_\phi(s)$ and determines the states where it should trust the demonstrated behavior, and the states where it should ignore the human’s actions.
- **Sasaki** [30]: A behavior cloning variant that shifts the learned policy towards the mode of the distribution. For this approach we set $R(s, a) = \pi_{prev}(a | s)$, the policy trained at the previous iteration. In practice **Sasaki** learns to emulate the human’s actions at states where the demonstrations are consistent, and ignores the human’s actions with high variability.

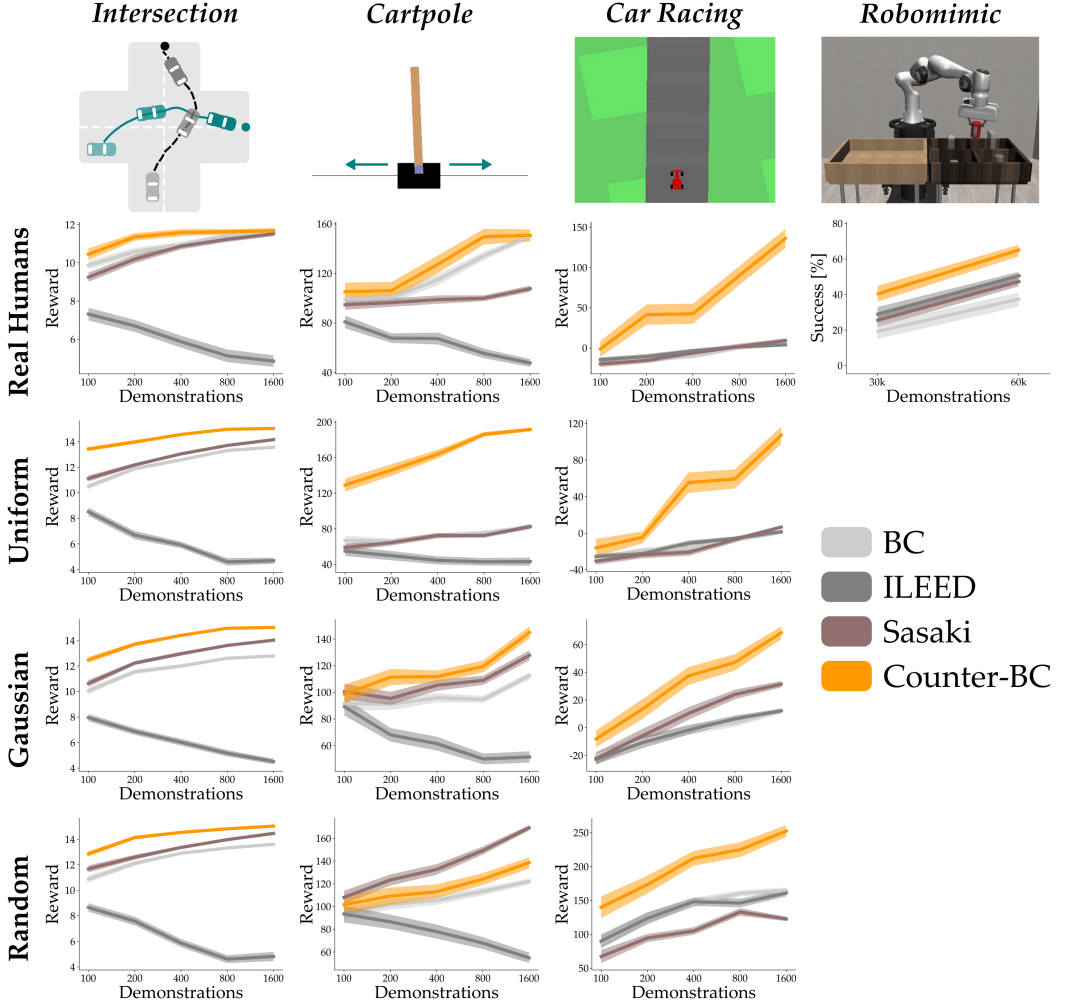


Fig. 4. Learning from real and simulated humans (see Sections 5.1 and 5.2). Every column shows a different environment, and the rows correspond to demonstrations from real humans, or synthetic operators with uniform, Gaussian, and random noise. Plots illustrate the performance of the policy learned by each algorithm as a function of the number of demonstrated state-action pairs (higher reward or success is better). For *Robomimic* we tested the *Can* task with standardized demonstrations from the Multi-Human dataset [27]. Results are averaged across 50 runs; shaded regions show standard error.

Note that we did not include offline reinforcement learning algorithms since the robot learner does not have access to the task reward, and thus these methods cannot be applied to our setting. In our implementation Counter-BC and the baselines are instantiated as Gaussian policies with two hidden layers of the same size. The learning rate, batch size, and number of epochs are held constant across all methods to mitigate against biased results.

5.1 How Does Counter-BC Perform with Different Types of Imperfect Demonstrations?

The results of our first simulation are shown in Figure 4. Each row of this figure corresponds to a different type of human demonstrator: actual participants, and then synthetic teachers with uniform,

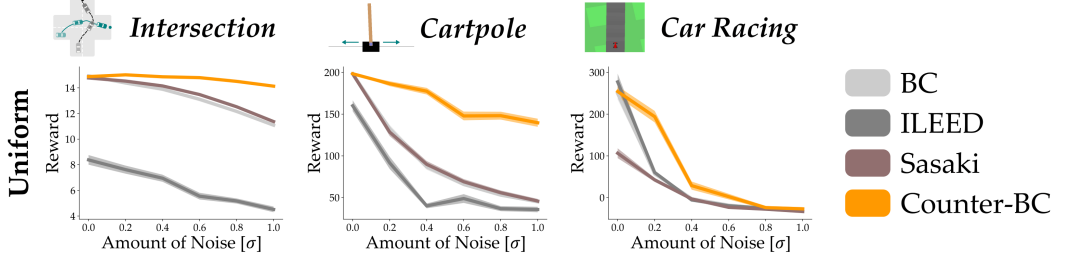


Fig. 5. Learning from increasingly noisy demonstrations (see Section 5.3). To regulate the amount of noise, we simulated a human teacher. This teacher selected actions $a = a^* + \epsilon$, where a^* is the optimal action and $\epsilon \sim \mathcal{U}(-\sigma, \sigma)$ is uniform noise. Increasing σ led to more noisy, imperfect, and suboptimal human teaching. The policies learned by each algorithm degrade as σ increases, but **Counter-BC** is more robust than the baselines. Results are averaged across 50 runs with demonstrations containing 400 state-action pairs.

Gaussian, or random noise. For the *Robomimic* environment we only collect data from real humans by leveraging the standardized dataset in [27]. In general, we observe that **Counter-BC** learns more proficient policies than the baselines. We particularly highlight the performance of **Counter-BC** in the *Car Racing* environment — where the control policies are based on image observations, and not direct state measurements — as well as the performance across environments with real human demonstrations. By contrast, the one type of imperfect demonstration where **Counter-BC** does not consistently reach the highest reward is random noise; here **Sasaki** occasionally outperforms **Counter-BC**. This result makes sense because **Sasaki** is designed to work with random noise. More specifically, **Sasaki** trains the policy so that it is better aligned with the human teacher’s most common actions — and when our simulated humans have random noise, their most common action is the optimal action a^* . For all other types of imperfect demonstrations we find **Counter-BC** leads to improved performance. Taken together, this suggests that **Counter-BC** learns the intended task despite controlled noise or uncontrolled errors in the human’s demonstrations.

5.2 How Does Counter-BC Perform with an Increasing Number of Demonstrations?

Within Figure 4 we also measure how the performance of each algorithm changes with varying amounts of human data. The number of demonstrated state-action pairs is shown along the x -axis of each individual plot. Intuitively, we would expect the system to perform better when given more examples: the more times the human shows the robot how to act, the more proficiently it should behave during rollouts. Our results affirm this intuition. Additionally, we see that **Counter-BC** outperforms the alternatives across different levels of demonstrations. This indicates that **Counter-BC** is not limited to scenarios where robots only have access to small amounts of data — **Counter-BC** can be more generally applied to large or small datasets.

5.3 How Does Counter-BC Perform with Varying Levels of Noise?

So far we have varied the type of human teacher and the amount of data; next, we adjust the level of noise within the human’s examples. Figure 5 corresponds to a setting where the robot is learning from increasingly suboptimal and imperfect demonstrations. When $\sigma = 0$ the synthetic human teacher perfectly demonstrates the task with optimal actions a^* , and as σ increases the human deviates from the optimal actions with uniform noise $\epsilon \sim \mathcal{U}(-\sigma, \sigma)$. Within the *Intersection*, *Cartpole*, and *Car Racing* environments the maximum magnitude of an action dimension is 1; hence, $\sigma = 1$ means that the size of the noise matches or exceeds the size of the optimal actions. We find that — relative to the baselines — **Counter-BC** is increasingly robust as σ grows and the synthetic

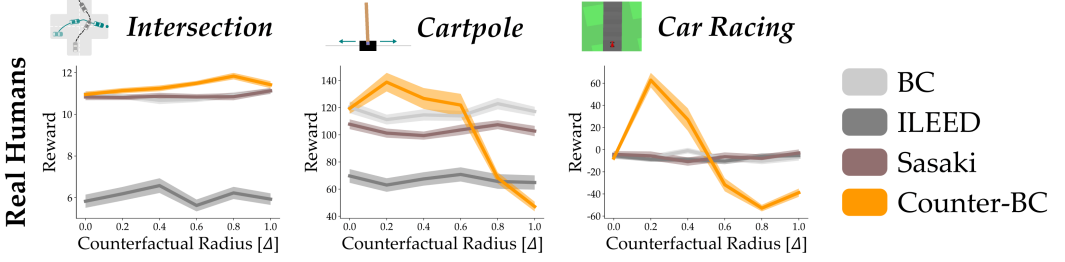


Fig. 6. Learning from demonstrations while varying hyperparameter Δ (see Section 5.4). Note that the hyperparameter Δ only applies to **Counter-BC**. Consistent with our theoretical analysis from Section 4.2, when $\Delta = 0$ then **Counter-BC** is equivalent to **BC**. Increasing Δ enlarges the counterfactual sets and leads to simpler explanations of the human’s demonstrations. Once Δ is increased too much, the robot begins to oversimplify the underlying human policy, resulting in degraded performance. Shaded regions show the standard error across 50 end-to-end runs with demonstrations that have 400 state-action pairs. These demonstrations were collected from $N = 20$ in-person participants.

human’s demonstrations become more noisy and suboptimal. When the human’s demonstrations have no noise ($\sigma \rightarrow 0$) then each method is roughly equivalent. But as the size of the noise increases ($\sigma \rightarrow 1$) we see the advantages of **Counter-BC** in reasoning over counterfactual actions, searching for simple policy explanations, and extrapolating the underlying task.

5.4 How Does Adjusting Hyperparameter Δ Affect Counter-BC?

We conclude our simulations by testing the effect of hyperparameter Δ on **Counter-BC**. In Section 4.2 and Figure 3 we theoretically showed that $\Delta \rightarrow 0$ causes the robot to exactly imitate all of the human’s actions, reducing **Counter-BC** to standard **BC**. Conversely, as Δ increases the robot should learn simpler functions by imitating actions close to (but not the same as) the behaviors actually demonstrated by the human teacher, resulting in learning capabilities beyond the current state-of-the-art. In Figure 6 we put this theory to the test with real human data. For datasets from $N = 20$ participants in *Intersection*, *Cartpole*, and *Car Racing*, we learn robot policies while adjusting the value of Δ . As expected, when $\Delta = 0$ the performance of **Counter-BC** equals the behavior of **BC**. Increasing Δ enables **Counter-BC** to expand the human’s demonstrations and extrapolate underlying functions, improving performance of the learned policy. However, when Δ is increased too far the robot eventually recovers policies that are simpler than what the human intended (i.e., missing nuances in the correct behavior), harming the performance of the autonomous robot. This suggests both a trade-off and guidelines for implementation. We recommend that designers start with low values of Δ , and gradually increase that hyperparameter to improve performance. We also recognize that one downside of **Counter-BC** is that — if designers initialize with values of Δ that significantly exceed the noise in the teacher’s demonstrations — the performance of our algorithm may actually fall below the **BC** baseline.

6 USER STUDY

Our previous experiments focused on simulated environments with real and synthetic human teachers. In our final study, we now test Counter-BC on a real-world robot arm (Franka FR3) with demonstrations provided by $N = 20$ in-person participants. The task matches our running example from Figure 1: human teachers teleoperate the robot arm to repeatedly hit an air hockey puck across a table. Based on the participants’ demonstrations, the robot must learn to align its paddle

with the oncoming puck, and then move forward to strike that puck with the correct timing. See examples of this game in our supplemental video: <https://youtu.be/XaeOZWht68>

Experimental Setup. Our experiment has two phases: training and testing. During *training* each individual participant sits next to the robot and uses a joystick to teleoperate the arm in real-time. The arm’s end-effector is constrained to move along the planar surface of an air hockey table. A red puck glides along this table; participants try to control the robot to hit that puck so it bounces off the opposite side and returns towards the robot arm. Based on the speed and location where participants hit the puck, the puck may move at various angles and velocities (e.g., colliding with the table’s sides). Hence, each iteration naturally forces users to vary the way they move the robot arm. These participants are not perfect teachers — their demonstrations include examples where they miss the puck entirely or accidentally hit it off-center.

Throughout training the robot records the position of the puck with an overhead camera (see Figure 7, Left). The robot also saves its end-effector locations and the user’s commanded actions. Overall, the robot’s state $s \in \mathbb{R}^6$ consists of the x - y position of its end-effector, the x - y position of the puck at the current timestep, and the puck’s x - y position at the previous timestep. Actions $a \in \mathbb{R}^2$ are end-effector velocities along the surface of the table normalized between 0 and 1. Each timestep of training yields a new (s, a) pair for dataset \mathcal{D} . After the participants’ demonstrations are completed, we move to the *testing* phase. Here the robot learns a control policy from the aggregated dataset \mathcal{D} and then rolls out this learned policy to autonomously play air hockey. We evaluate the proficiency of the robot’s control policy across multiple interactions.

Independent Variables. During testing we modulate two variables: the *algorithm* the robot uses to learn its control policy, and the *amount of data* leveraged by that algorithm. We compare the same offline imitation learning methods as in Section 5. These include our proposed **Counter-BC** approach, as well as state-of-the-art baselines **BC** [19], **ILEED** [2], and **Sasaki** [30]. Each algorithm learns from the same human demonstrations. We sample these demonstrations from the aggregated dataset \mathcal{D} collected during training; specifically, we measure the robot’s performance when trained on 200, 400, 800, 1600, and 3200 state-action pairs.

Dependent Measures. We rollout each learned policy in the air hockey environment. Ideally, the robot will learn to repeatedly hit the puck while moving quickly and efficiently. We therefore count the *Number of Hits*, i.e., the number of times the robot uses its end-effector to push the puck towards the opposite end of the table. To assess efficiency, we record the *Distance per Hit*. This corresponds to the distance the robot’s end-effector travels during an interaction (in meters) divided by the number of hits; if the robot never hits the puck, then this is just the total distance traveled. Similarly, the *Time per Hit* is the total interaction time (in seconds) divided by the number of hits. As before, if the robot never hits the puck, *Time per Hit* becomes the total interaction time. A proficient robot should repeatedly hit the puck (maximizing *Number of Hits*) while minimizing the distance traveled (*Distance per Hit*) and the time between hits (*Time per Hit*).

Participants and Procedure. A total of $N = 20$ users provided demonstrations for the air hockey task (3 female, average age 24 ± 4 years). These were the same users that taught the simulated robots in Section 5. After giving informed written consent (IRB #23-1237), participants practiced teleoperating the robot arm with a joystick for 2 to 5 minutes. Users then controlled the robot to play air hockey for 2 minutes of recorded demonstrations. We aggregate the data from all 20 users into a single combined dataset \mathcal{D} , and uniformly randomly sample from this dataset to collect the state-action pairs need to train the robot learner.

During testing we perform 10 end-to-end runs for each learning algorithm and amount of data. In what follows we describe a single one of these runs. To evaluate the performance with k datapoints, we first sample k state-action pairs from dataset \mathcal{D} and then train all four algorithms with those

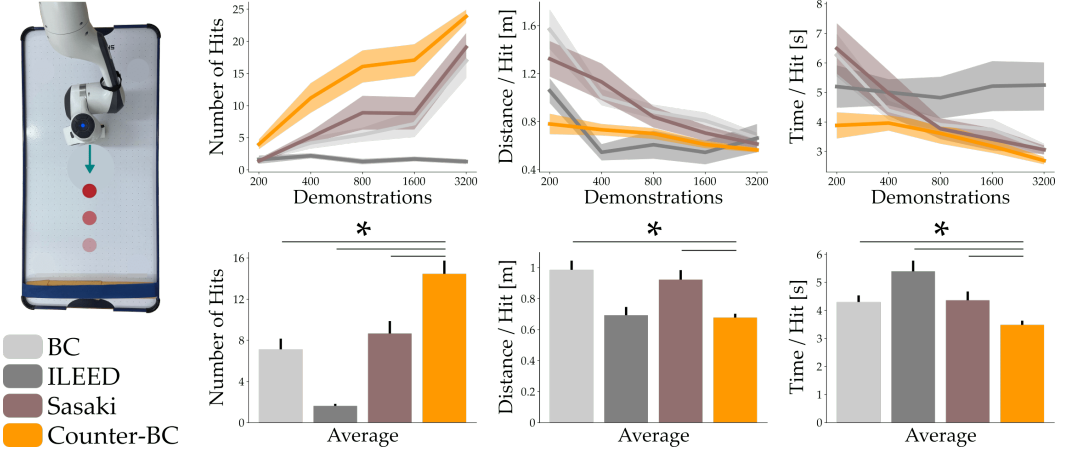


Fig. 7. Results from our air hockey experiment in Section 6. In-person participants provided demonstrations where they teleoperated the robot arm to repeatedly hit a hockey puck (also see Figure 1). The top row plots the performance of the robot’s learned policy when trained on an increasing number of state-action pairs; the bottom row shows the average performance across all dataset sizes. *Number of Hits* is the number of times the robot autonomously hit the puck (higher is better). *Distance per Hit* is path length of the robot’s end-effector divided by the number of hits (lower is better), and *Time per Hit* is the total interaction time divided by the number of hits (lower is better). Our results suggest that robots which use **Counter-BC** to learn from human demonstrations outperform other offline imitation learning approaches that account for imperfect teaching. Shaded regions and error bars show the standard error, and an * denotes statistical significance ($p < .05$).

same datapoints. For each method (**BC**, **ILEED**, **Sasaki**, **Counter-BC**) we then place the hockey puck directly in front of the robot’s end-effector and start executing the learned policy. We record the *Number of Hits*, *Distance per Hit*, and *Time per Hit* until the robot misses the puck and the puck comes to rest. Repeating this end-to-end process 10 times for all five levels of demonstration, we ultimately test each learning algorithm a total of 50 times.

Hypotheses. We hypothesized that:

*Robots that use **Counter-BC** to learn from human demonstrations will extract more proficient control policies than the baselines.*

Results. Our experimental results are summarized in Figure 7. In the top row we plot our dependent measures as a function of the number of demonstrations; the bottom row displays the average outcomes across all 50 trials for each algorithm. As a reminder, for the *Number of Hits* **higher** values indicate better task performance. By contrast, for the *Distance per Hit* and the *Time per Hit* **lower** values mean the robot is playing the game more quickly and efficiently.

To capture overall trends in the learned policies we will analyze the average results. Repeated measures ANOVAs with Greenhouse-Geisser corrections determine that algorithm type has a statistically significant effect on the *Number of Hits* ($F(2.74, 134.24) = 39.8, p < .001$), the *Distance per Hit* ($F(2.42, 118.78) = 12.6, p < .001$), and the *Time per Hit* ($F(1.89, 92.48) = 8.3, p < .001$). To better understand these differences, we next conduct post hoc tests with a Bonferroni adjustment. Here we see that **Counter-BC** averages a higher *Number of Hits* across all demonstrations as compared to **BC** ($p < .001$), **ILEED** ($p < .001$), and **Sasaki** ($p < .001$). Similarly, the *Time per Hit* for **Counter-BC** is lower than **BC** ($p < .01$), **ILEED** ($p < .001$), and **Sasaki** ($p < .05$). For the *Distance per Hit* we gather mixed findings: **Counter-BC** is again more performant than **BC** ($p < .001$) and **Sasaki** ($p < .01$), but comparisons with **ILEED** are not statistically significant

($p = 1.0$). We can explain this result by watching the learned behavior for **ILEED**. In our tests, robots trained with **ILEED** barely move the end-effector, often missing the puck or hitting that puck at a low velocity. Accordingly — although **ILEED** has a low *Distance per Hit* — it is not an effective policy for repeatedly hitting the puck and completing the desired task. We note that **ILEED** was originally designed for settings where there are multiple human teachers, and the robot knows which demonstrations belong to which teacher. The relatively poor performance of **ILEED** is likely because (in our setting) we do not assume any labels on the dataset, and so **ILEED** cannot connect individual datapoints with any specific human teacher.

In summary, our results from Figure 7 support our hypothesis and suggest that **Counter-BC** is an effective algorithm for learning from real human data on physical robot arms. Across each axis of evaluation (*Number of Hits*, *Distance per Hit*, and *Time per Hit*), we find that **Counter-BC** outperforms or matches the baselines, and these trends hold regardless of the number of state-action pairs leveraged to train the robot learner.

7 CONCLUSION

Existing imitation learning algorithms seek to emulate the exact actions of a human teacher. By contrast, this work introduced a different perspective. Our core hypothesis was that all of the human’s data is based on the underlying task they are trying to convey. Suboptimality inherent to human teaching adds unintended complexity to the dataset, but we can develop learning algorithms to work around this noise and recover the underlying function. In doing so, the robot is no longer constrained to imitate the human’s *exact* datapoints; instead, the robot can now propose and imitate *counterfactual* actions to reach a coherent, simple explanation of what the human meant. We formalized this concept by deriving Counter-BC, a novel offline imitation learning algorithm that accounts for imperfect human teachers. We proved that the loss function used to train Counter-BC generalized prior works; put another way, current methods can be viewed as instances of our overarching approach. In practice, by optimizing this generalized loss Counter-BC trains the policy to minimize entropy over actions (i.e., reaching a simple explanation) while ensuring that the actions output by the policy are close to the actions demonstrated by the human (i.e., remaining within the counterfactual set). Our analysis indicated that Counter-BC can extract the desired policy from imperfect data, multiple users, and teachers of varying skill. To support these findings, we tested Counter-BC across several environments with real human teachers, synthetic demonstrations, and standardized datasets. We note that our testing included learning tasks from images, learning tasks with high-dimensional states, and learning tasks on real-world robot arms. Results indicated that Counter-BC learns more proficient policies than state-of-the-art baselines. In particular, we found that Counter-BC is robust to different types of human data with varying levels of noise, and that Counter-BC is also more performant when trained on real human demonstrations. Overall, our theoretical and empirical contributions are a step towards robots that learn what their human teachers actually meant, not just what the human teacher showed.

Limitations. One advantage and disadvantage of Counter-BC is the hyperparameter $\Delta \geq 0$ in Algorithm 1. This hyperparameter specifies the size of the counterfactual set; intuitively, increasing Δ means the robot can extrapolate more from the human’s data, but the resulting policy may contain greater deviations from the human’s demonstrations. The advantage of Δ is that designers can tune this parameter along a continuous spectrum so that Counter-BC works with expert teachers (low values of Δ) and inexperienced teachers (high values of Δ). The disadvantage is that — if designers choose too large a Δ — Counter-BC may oversimplify the policy and miss important nuances in the task. Within our manuscript we tried to mitigate this potential issue by

presenting design guidelines and by testing with different Δ values. In future work, we would like to automate the selection of Δ based on the offline dataset of human demonstrations.

REFERENCES

- [1] Baris Akgun, Maya Cakmak, Karl Jiang, and Andrea L Thomaz. 2012. Keyframe-based learning from demonstration: Method and evaluation. *International Journal of Social Robotics* 4 (2012), 343–355.
- [2] Mark Beliaev, Andy Shih, Stefano Ermon, Dorsa Sadigh, and Ramtin Pedarsani. 2022. Imitation learning by estimating expertise of demonstrators. In *International Conference on Machine Learning*. 1732–1748.
- [3] Suneel Belkale, Yuchen Cui, and Dorsa Sadigh. 2023. Data quality in imitation learning. *Advances in Neural Information Processing Systems* 36 (2023), 80375–80395.
- [4] Kevin Black, Noah Brown, Danny Driess, Adnan Esmail, Michael Equi, Chelsea Finn, Niccolo Fusai, Lachy Groom, Karol Hausman, Brian Ichter, et al. 2024. π_0 : A Vision-Language-Action Flow Model for General Robot Control. *arXiv preprint arXiv:2410.24164* (2024).
- [5] Andreea Bobu, Andi Peng, Pulkit Agrawal, Julie A Shah, and Anca D Dragan. 2024. Aligning human and robot representations. In *ACM/IEEE International Conference on Human-Robot Interaction*. 42–54.
- [6] Daniel S Brown, Wonjoon Goo, and Scott Niekum. 2020. Better-than-demonstrator imitation learning via automatically-ranked demonstrations. In *Conference on Robot Learning*. 330–359.
- [7] Xingchen Cao, Fan-Ming Luo, Junyin Ye, Tian Xu, Zhilong Zhang, and Yang Yu. 2024. Limited preference aided imitation learning from imperfect demonstrations. In *International Conference on Machine Learning*.
- [8] Annie S Chen, Alec M Lessing, Yuejiang Liu, and Chelsea Finn. 2025. Curating Demonstrations using Online Experience. *arXiv preprint arXiv:2503.03707* (2025).
- [9] Letian Chen, Rohan Paleja, and Matthew Gombolay. 2021. Learning from suboptimal demonstration via self-supervised reward regression. In *Conference on Robot Learning*. 1262–1277.
- [10] Sirui Chen, Chen Wang, Kaden Nguyen, Li Fei-Fei, and C Karen Liu. 2024. ARCap: Collecting high-quality human demonstrations for robot learning with augmented reality feedback. *arXiv preprint arXiv:2410.08464* (2024).
- [11] Sonia Chernova and Andrea L Thomaz. 2022. *Robot Learning from Human Teachers*. Springer Nature.
- [12] Yinlong Dai, Robert Ramirez Sanchez, Ryan Jeronimus, Shahabedin Sagheb, Cara M Nunez, Heramb Nemlekar, and Dylan P Losey. 2025. CIVIL: Causal and Intuitive Visual Imitation Learning. *arXiv preprint arXiv:2504.17959* (2025).
- [13] Pete Florence, Corey Lynch, Andy Zeng, Oscar A Ramirez, Ayzaan Wahid, Laura Downs, Adrian Wong, Johnny Lee, Igor Mordatch, and Jonathan Tompson. 2022. Implicit behavioral cloning. In *Conference on Robot Learning*. 158–168.
- [14] Kanishk Gandhi, Siddharth Karamcheti, Madeline Liao, and Dorsa Sadigh. 2023. Eliciting compatible demonstrations for multi-human imitation learning. In *Conference on Robot Learning*. 1981–1991.
- [15] Udit Ghosh, Dripta S Raychaudhuri, Jiachen Li, Konstantinos Karydis, and Amit K Roy-Chowdhury. 2024. Robust offline imitation learning from diverse auxiliary data. *arXiv preprint arXiv:2410.03626* (2024).
- [16] Jake Grigsby and Yanjun Qi. 2021. A closer look at advantage-filtered behavioral cloning in high-noise datasets. *arXiv preprint arXiv:2110.04698* (2021).
- [17] Soheil Habibian, Antonio Alvarez Valdivia, Laura H Blumenschein, and Dylan P Losey. 2025. A survey of communicating robot learning during human-robot interaction. *The International Journal of Robotics Research* 44, 4 (2025), 665–698.
- [18] Joey Hejna, Suvir Mirchandani, Ashwin Balakrishna, Annie Xie, Ayzaan Wahid, Jonathan Tompson, Pannag Sanketi, Dhruv Shah, Coline Devin, and Dorsa Sadigh. 2025. Robot Data Curation with Mutual Information Estimators. *arXiv preprint arXiv:2502.08623* (2025).
- [19] Liyiming Ke, Sanjiban Choudhury, Matt Barnes, Wen Sun, Gilwoo Lee, and Siddhartha Srinivasa. 2021. Imitation learning as f-divergence minimization. In *Workshop on the Algorithmic Foundations of Robotics*. 313–329.
- [20] Alexander Khazatsky, Karl Pertsch, Suraj Nair, Ashwin Balakrishna, Sudeep Dasari, Siddharth Karamcheti, Soroush Nasiriany, Mohan Kumar Srirama, Lawrence Yunliang Chen, Kirsty Ellis, et al. 2024. DROID: A large-scale in-the-wild robot manipulation dataset. In *Robotics: Science and Systems*.
- [21] Geon-Hyeon Kim, Seokin Seo, Jongmin Lee, Wonseok Jeon, Hyeonjoo Hwang, Hongseok Yang, and Kee-Eung Kim. 2021. DemoDICE: Offline imitation learning with supplementary imperfect demonstrations. In *International Conference on Learning Representations*.
- [22] Sachit Kuhar, Shuo Cheng, Shivang Chopra, Matthew Bronars, and Danfei Xu. 2023. Learning to discern: Imitating heterogeneous human demonstrations with preference and representation learning. In *Conference on Robot Learning*. 1437–1449.
- [23] Aviral Kumar, Joey Hong, Anikait Singh, and Sergey Levine. 2022. When should we prefer offline reinforcement learning over behavioral cloning? *arXiv preprint arXiv:2204.05618* (2022).
- [24] Ziniu Li, Tian Xu, Zeyu Qin, Yang Yu, and Zhi-Quan Luo. 2023. Imitation learning from imperfection: Theoretical justifications and algorithms. *Advances in Neural Information Processing Systems* 36 (2023), 18404–18443.

- [25] Dylan P Losey, Andrea Bajcsy, Marcia K O'Malley, and Anca D Dragan. 2022. Physical interaction as communication: Learning robot objectives online from human corrections. *The International Journal of Robotics Research* 41, 1 (2022), 20–44.
- [26] Dylan P Losey, Hong Jun Jeon, Mengxi Li, Krishnan Srinivasan, Ajay Mandlekar, Animesh Garg, Jeannette Bohg, and Dorsa Sadigh. 2022. Learning latent actions to control assistive robots. *Autonomous Robots* 46, 1 (2022), 115–147.
- [27] Ajay Mandlekar, Danfei Xu, Josiah Wong, Soroush Nasiriany, Chen Wang, Rohun Kulkarni, Li Fei-Fei, Silvio Savarese, Yuke Zhu, and Roberto Martin-Martin. 2021. What matters in learning from offline human demonstrations for robot manipulation. *arXiv preprint arXiv:2108.03298* (2021).
- [28] Shaunak A Mehta, Yusuf Umut Ciftci, Balamurugan Ramachandran, Somil Bansal, and Dylan P Losey. 2025. Stable-BC: Controlling covariate shift with stable behavior cloning. *IEEE Robotics and Automation Letters* (2025).
- [29] Maram Sakr, Zhikai Zhang, Benjamin Li, Haomiao Zhang, HF Van der Loos, Dana Kulic, and Elizabeth Croft. 2023. How can everyday users efficiently teach robots by demonstrations? *arXiv preprint arXiv:2310.13083* (2023).
- [30] Fumihiro Sasaki and Ryota Yamashina. 2020. Behavioral cloning from noisy demonstrations. In *International Conference on Learning Representations*.
- [31] Aran Sena and Matthew Howard. 2020. Quantifying teaching behavior in robot learning from demonstration. *The International Journal of Robotics Research* 39, 1 (2020), 54–72.
- [32] Jonathan Spencer, Sanjiban Choudhury, Matthew Barnes, Matthew Schmitt, Mung Chiang, Peter Ramadge, and Sidd Srinivasa. 2022. Expert intervention learning: An online framework for robot learning from explicit and implicit human feedback. *Autonomous Robots* (2022), 1–15.
- [33] Zexu Sun, Bowei He, Jinxin Liu, Xu Chen, Chen Ma, and Shuai Zhang. 2023. Offline imitation learning with variational counterfactual reasoning. *Advances in Neural Information Processing Systems* (2023), 43729–43741.
- [34] Voot Tangkaratt, Bo Han, Mohammad Emtiyaz Khan, and Masashi Sugiyama. 2020. Variational imitation learning with diverse-quality demonstrations. In *International Conference on Machine Learning*. 9407–9417.
- [35] Octo Model Team, Dibya Ghosh, Homer Walke, Karl Pertsch, Kevin Black, Oier Mees, Sudeep Dasari, Joey Hejna, Tobias Kreiman, Charles Xu, et al. 2024. Octo: An open-source generalist robot policy. *arXiv preprint arXiv:2405.12213* (2024).
- [36] Mark Towers, Ariel Kwiatkowski, Jordan Terry, John U Balis, Gianluca De Cola, Tristan Deleu, Manuel Goulao, Andreas Kallinteris, Markus Krimmel, Arjun KG, et al. 2024. Gymnasium: A standard interface for reinforcement learning environments. *arXiv preprint arXiv:2407.17032* (2024).
- [37] Antonio Alvarez Valdivia, Soheil Habibian, Carly A Mendenhall, Francesco Fuentes, Ritish Shailly, Dylan P Losey, and Laura H Blumenschein. 2023. Wrapping haptic displays around robot arms to communicate learning. *IEEE Transactions on Haptics* 16, 1 (2023), 57–72.
- [38] Qiang Wang, Robert McCarthy, David Cordova Bulens, Kevin McGuinness, Noel E O'Connor, Francisco Roldan Sanchez, Nico Gürtler, Felix Widmaier, and Stephen J Redmond. 2023. Improving behavioural cloning with positive unlabeled learning. In *Conference on Robot Learning*. 3851–3869.
- [39] Qiang Wang, Robert McCarthy, David Cordova Bulens, Francisco Roldan Sanchez, Kevin McGuinness, Noel E O'Connor, and Stephen J Redmond. 2023. Identifying expert behavior in offline training datasets improves behavioral cloning of robotic manipulation policies. *IEEE Robotics and Automation Letters* 9, 2 (2023), 1294–1301.
- [40] Yunke Wang, Chang Xu, Bo Du, and Honglak Lee. 2021. Learning to weight imperfect demonstrations. In *International Conference on Machine Learning*. 10961–10970.
- [41] Yueh-Hua Wu, Nontawat Charoenphakdee, Han Bao, Voot Tangkaratt, and Masashi Sugiyama. 2019. Imitation learning from imperfect demonstration. In *International Conference on Machine Learning*. 6818–6827.
- [42] Haoran Xu, Xianyu Zhan, Honglei Yin, and Huiling Qin. 2022. Discriminator-weighted offline imitation learning from suboptimal demonstrations. In *International Conference on Machine Learning*. 24725–24742.
- [43] Mengjiao Yang, Sergey Levine, and Ofir Nachum. 2021. TRAIL: Near-Optimal Imitation Learning with Suboptimal Data. In *International Conference on Learning Representations*.
- [44] Sheng Yue, Jiani Liu, Xingyuan Hua, Ju Ren, Sen Lin, Junshan Zhang, and Yaoxue Zhang. 2024. How to leverage diverse demonstrations in offline imitation learning. In *International Conference on Machine Learning*.
- [45] Maryam Zare, Parham M Kebria, Abbas Khosravi, and Saeid Nahavandi. 2024. A survey of imitation learning: Algorithms, recent developments, and challenges. *IEEE Transactions on Cybernetics* (2024).
- [46] Songyuan Zhang, Zhangjie Cao, Dorsa Sadigh, and Yanan Sui. 2021. Confidence-aware imitation learning from demonstrations with varying optimality. *Advances in Neural Information Processing Systems* 34 (2021), 12340–12350.
- [47] Konrad Zolna, Alexander Novikov, Ksenia Konyushkova, Caglar Gulcehre, Ziyu Wang, Yusuf Aytar, Misha Denil, Nando de Freitas, and Scott Reed. 2020. Offline learning from demonstrations and unlabeled experience. In *Offline Reinforcement Learning Workshop at Neural Information Processing Systems*.